THE JOURNAL OF BIOLOGICAL CHEMISTRY
Vol. 272, No. 21, Issue of May 23, pp. 13666–13675, 1997

Printed in U.S.A.

Functional Evaluation of the Structural Features of Proteases and Their Substrate in Fibrin Surface Degradation*

(Received for publication, November 20, 1996, and in revised form, February 21, 1997)

Krasimir Kolev, Kiril Tenekedjiev‡, Erzsébet Komorowicz, and Raymund Machovich§

From the Department of Medical Biochemistry, Semmelweis University of Medicine, H-1088 Budapest, Hungary

A new model has been introduced to characterize the action of a fluid phase enzyme on a solid phase substrate. This approach is applied to evaluate the kinetics of fibrin dissolution with several proteases. The model predicts the rate constants for the formation and dissociation of the protease-fibrin complex, the apparent order of the association reaction between the enzyme and the substrate, as well as a global catalytic constant (k_{cat}) for the dissolution process. These kinetic parameters show a strong dependence on the nature of the applied protease and on the structure of the polymerized substrate. The kinetic data for trypsin, PMN-elastase, and three plasminogen-derived proteases with identical catalytic domain, but with a varied N-terminal structure, are compared. The absence of kringle$_5$ in des-kringle$_{1-5}$-plasmin (microplasmin) is related to a markedly lower k_{cat} (0.008 s^{-1}) compared with plasmin and des-kringle$_{1-4}$-plasmin (miniplasmin) (0.039 s^{-1}). The essentially identical kinetic parameters for miniplasmin and plasmin with the exception of k_{diss}, which is higher for miniplasmin (81.8 s^{-1} *versus* 57.6 s^{-1}), suggest that the first four kringle domains are needed to retain the enzyme in the enzyme-fibrin complex. Trypsin, a protease of similar primary specificity to plasmin, but with a different catalytic domain, shows basically the same k_{cat} as plasmin, but its affinity to fibrin is markedly lower compared with plasmin and even microplasmin. The latter suggests that in addition to the kringle domains, the structure of the catalytic domain in plasmin also contributes to its specificity for fibrin. The thinner and extensively branched fibers of fibrin are more efficiently dissolved than the fibers with greater diameter and lower number of branching points. When the polymer is stabilized through covalent cross-linking, the k_{cat} for plasmin and miniplasmin is 2–4-fold higher than on non-cross-linked fibrin, but the decrease in the association rate constant for the formation of enzyme-substrate complex explains the relative proteolytic resistance of the cross-linked fibrin. Thus, the functional evaluation of the discrete steps of the fibrinolytic process reveals new aspects of the interactions between proteases and their polymer substrate.

The complex network of blood coagulation culminates in the conversion of fibrinogen to the rod-shaped fibrin monomers (for review, see Ref. 1). The non-covalent interactions among the fibrin monomers result in the formation of long double-stranded polymers in which the protomeric units are positioned in a half-staggered manner. Factors that influence the rate of the conversion of fibrinogen to fibrin and the strength of the polymerization interactions determine the final fiber diameter and clot structure. Increase in the NaCl concentration or in the pH reduces the number of protofibrils in a single fiber and the porosity of the fibrin network (2, 3); *e.g.* as the NaCl concentration is changed from 50 to 400 mM, the fiber diameter decreases from 180 to 39 nm, and the average distance between two branching points of the network falls from 1690 to 93 nm. Lowering the concentration of fibrinogen, the rate of its conversion to fibrin, and the presence of Ca^{2+} increases the fiber diameter and the porosity of the gel (4, 5). The structural features of the fibrin gel affect the physicochemical properties of fibrin (permeability and light scattering) (4, 5), but their influence on the susceptibility of fibrin to proteolytic enzymes has not been quantitatively characterized. The structure of fibrin is covalently modified by the activated factor XIII that inserts isopeptide bonds between fibrin monomers (for review, see Ref. 6). The functional aspects of this modification with respect to proteolytic susceptibility are documented. The cross-linking renders fibrin relatively resistant to degradation with plasmin (7–10) and leukocyte proteases (11, 12), but exact quantitative evaluation of this relative resistance has not been performed.

The serine protease plasmin is generally considered to be the enzyme responsible for the dissolution of fibrin clots under physiological and pathological conditions (for review, see Ref. 13). Morphological data for the presence of polymorphonuclear neutrophils in thrombi (14, 15), the immunochemical detection of specific fibrinogen degradation products in plasma samples *in vivo* (16), and the identification of PMN-elastase[1] and cathepsin-G as the major fibrinolytic enzymes of polymorphonuclear leukocytes (17) suggested a concept for an alternative fibrinolytic pathway (18, and for review, see Ref. 19). According to this concept, in addition to plasmin and PMN-proteases, a fibrinolytic role is attributed to miniplasmin,[2] which is generated after activation of the elastase-degraded form of plasminogen (M_r 38,000) lacking four of the five kringle domains that represent the N-terminal Glu^1-Val^{441} sequence of plasminogen (20). The catalytic properties of some of these proteases have been evaluated in homogeneous systems for fibrinogen as a substrate (21, 22) or for fibrin with enzymes dispersed within the clot (23). According to these kinetic data plasmin, miniplas-

* This work was supported in part by Hungarian Grants OTKA-T016497, ETT 383/1993, and ETK-I11/95 and by the U. S.-Hungarian Joint Fund Grant 449/95. The costs of publication of this article were defrayed in part by the payment of page charges. This article must therefore be hereby marked "*advertisement*" in accordance with 18 U.S.C. Section 1734 solely to indicate this fact.

‡ On leave from Varna Polytechnical University, Varna, Bulgaria.

§ To whom correspondence should be addressed: Semmelweis University of Medicine, Dept. of Medical Biochemistry, Puskin u. 9., H-1444, Budapest, P.O.Box 262, Hungary. Tel.: 36-1 266 1030; Fax: 36-1 266 7480.

[1] In this paper, the serine protease elastase (M_r 30,000), found in the azurophil granules of the neutrophil polymorphonuclear leukocytes, is referred to as PMN-elastase.

[2] The abbreviations used are: miniplasmin, des-kringle$_{1-4}$-plasmin; PMSF, phenylmethylsulfonyl fluoride; 6AH, 6-aminohexanoate; microplasmin, des-kringle$_{1-5}$-plasmin.

min and PMN-elastase are the most efficient fibrinolytic enzymes, and a conclusion is drawn that the high affinity lysine binding site in the N-terminal kringle domains of plasmin is involved in the interactions with the native polymerized fibrin, whereas the fifth kringle found in both enzymes participates in binding to lysine residues newly exposed in the course of fibrin degradation (23).

Two possible access routes to the fibrin substrate exist for an enzyme (24), an intrinsic one (when the protease is entrapped within the fibrin network) and an extrinsic one (when the fluid phase-borne enzyme attacks the surface of the clot). Since even contracted blood clots do not hinder the free diffusion of particles with M_r up to 470,000 (25) in the former case, classical approaches can be used for the kinetic evaluation of the fibrinolytic proteases if the enzymes are uniformly dispersed within the clot (23). In the second case, the catalysis at a phase interface introduces major complications into enzyme kinetics. The extrinsic access route for fibrin, however, is of primary physiological importance since the blood-borne plasminogen activators and plasminogen assemble on the surface of the clot or propagate into it (for review, see Refs. 13 and 26), and the neutrophil leukocytes adhere to this surface (27, 28) where the generated or released proteases are protected against the plasma-derived protease inhibitors (29). Consequently, it is an intriguing task to characterize with exact kinetic data the proteolytic events at this interface. The complex character of the problem comes from the high heterogeneity of the system. The interface surface contains a relatively limited number of enzyme-susceptible cleavage sites. Thus, the fluid phase-borne protease binds to nonspecific sites of the substrate surface (absorption) or, less frequently, directly attacks the cleavage-sites. After the absorption, the enzyme can approach the susceptible site through lateral movement along the fiber (first change in the dimensionality of the reaction), or, alternatively, it can move into the fiber (a second change in the dimensionality), desorb into the fluid phase, or move into the inner pores of the gel. Consequently, the kinetic evaluation of the overall rate of fibrin dissolution should consider the relative rates of these movements, the changes in the dimensionality, and the rate of the hydrolytic reactions. In similar systems where degradation of different biopolymers or phospholipids occurs on phase interface, special mathematical approaches have been introduced for kinetic characterization of the hydrolytic events (30–36). Recently, elaborate models have been developed for the evaluation of fibrin dissolution, which take into account the details of the transport phenomena (37–39). According to these data, the diffusion of fibrin-binding proteins into the clot is severely impaired, which results in accumulation of the extrinsically applied enzyme in a thin superficial layer of the gel. Morphological data confirm that the lytic process is restricted to a several micrometer deep zone at the surface of the clot (40, 41). In the present study, we introduce a new model for the kinetics of fibrin surface degradation with proteases and apply it for the comparison of several fibrinolytic enzymes and for the evaluation of the impact of fibrin and enzyme structure on the lytic process. Further insights into the structure-function relationship of the fibrinolytic proteases can be gained from the kinetic behavior of trypsin (a protease of similar primary specificity to plasmin) and of a lower molecular weight derivative of plasmin, microplasmin (M_r 29,000) lacking all kringle domains (42, 43).

EXPERIMENTAL PROCEDURES

Human plasma was collected from healthy volunteers. Streptokinase, aprotinin, porcine pancreatic elastase, Factor XIIIa (from human placenta), and the chromogenic elastase substrate (methoxysuccinyl-L-alanyl-L-alanyl-L-prolyl-L-valine-*p*-nitroanilide) were from Calbiochem (La Jolla, CA). The chromogenic plasmin substrate Spectrozyme-PL (H-D-norleucyl-hexahydrotyrosyl-lysine-*p*-nitroanilide) was a product of American Diagnostica (Hartford, CT). Human fibrinogen was purchased from Chromogenix AB (Mölndal, Sweden). Lysine-Sepharose 4B, Sephadex G-25, and Sephacryl S-400 HR were from Pharmacia Biotech Inc. (Uppsala, Sweden). PMN-elastase, human thrombin (1000 NIH units/mg), *p*-nitrophenyl *p′*-guanidinobenzoate and phenylmethylsulfonyl fluoride were the products of Sigma. Bovine serum albumin and bovine pancreas trypsin were from Serva (Heidelberg, Germany), lactoperoxidase and 4-(2-aminoethyl)-benzenesulfonyl fluoride (Pefabloc®) were from Boehringer Mannheim (Germany). $Na^{125}I$ (carrier-free) was purchased from Izinta Ltd. (Budapest, Hungary). All other reagents were purchased from Reanal (Budapest, Hungary).

Plasminogen, Miniplasminogen, and Microplasmin Preparation—Published procedures were used for their isolation from citrated human plasma and further purification (20, 42, 44).

Plasmin and Miniplasmin Generation, Determination of Active Enzyme Concentration—These were performed as described previously for plasmin, miniplasmin, and PMN-elastase (29). The concentration of microplasmin and trypsin was determined with active-site titration (45).

Fibrinogen Purification and Fibrin Formation—Plasminogen-free fibrinogen with no contaminant factor XIII activity was prepared from freeze-dried human fibrinogen as described previously (23). In a microplate well, 200 μl of the purified fibrinogen (2 g/l) in 10 mM imidazole buffer, pH 7.4, containing 3 mM Ca^{2+} and varying amounts of NaCl was clotted with 1 NIH unit/ml thrombin to gain non-cross-linked fibrin. It has recently been shown (46) that the Cl^- concentration determines the structure of the polymerizing fibrin and not the ionic strength of the solution as it was previously believed (2). For the preparation of cross-linked fibrin, the inactivation of factor XIII was omitted from the purification procedure of fibrinogen, and, after clotting as above, fibrin was completely cross-linked in 16 h by the contaminant factor XIII as evidenced by gel electrophoresis.

Basic Interrelations in the Model of Fibrin Surface Degradation—A fibrinolytic enzyme in a homogeneous solution is applied to the surface of the preformed fibrin gel in a microplate well, and the turbidity of the clot that reflects the mass/length ratio of the fibrin fibers (23) is followed by measuring A_{340} with a Dynatech MR 5000 microplate reader. In the course of clot dissolution, the turbidity decreases due to reduction in the mass/length ratio of the fibrin fibers, resulting in solubilization in the interface layer and consumption of the gel phase. When a fluid phase-borne protease reaches the surface of the fibrin-gel, the enzyme molecules diffuse through the interface of the two phases and bind to the surface of the fibrin fibers either at proteolysis-susceptible sites or at nonspecific sites. In the former case, the protease molecules catalyze hydrolysis of peptide bonds in the fibrin, whereas, in the latter case, they migrate along the fibers to the cleavable bond or dissociate without hydrolytic effect (ineffective binding) and further diffuse among the fibrin fibers or into the fibers (internal diffusion). According to our measurements (see "Results") and to the experimental data of others (37–41), no significant diffusion is expected for molecules that specifically bind to fibrin. Consequently, it is reasonable to assume the existence of a reactive boundary layer to which the dissolution process is restricted (see Fig. 1). The depth of this layer does not depend on the concentration of the applied enzyme, and the enzyme concentration in it is approximately 10-fold higher than in the bulk phase (40, 41). For the sake of generality (to eliminate the dependence of the parameters on the actual size of the examined surface), we restrict the evaluation of the dissolution reaction to a subvolume V_x of the reactive boundary layer with surface area $S = 1$ [−] (see Fig. 1). The basic process in this layer can be described,

$$E(\tau) + F_l \underset{k_{-1}}{\overset{k_1}{\rightleftharpoons}} EF \xrightarrow{k_2} E(\tau) + P(\tau) \qquad \text{(Eq. 1)}$$

where $E(\tau)$ is the number of free enzyme molecules at time τ in V_x, F_l is the number of substrate molecules in the boundary layer that are available for degradation in V_x, EF is the number of enzyme-substrate complexes in V_x and $P(\tau)$ is the number of degraded substrate molecules per unit surface of the boundary layer. Our experiments indicate that enzyme activity is not influenced by increase in degradation product concentration; the final degradation products added at the maximal concentration for this system do not change the enzyme activity (not shown). Thus, the rate of formation of EF complex [nmol/m^2] can be described by the following equation where r [m] is the depth of the hypothetical reactive boundary layer (Fig. 1).

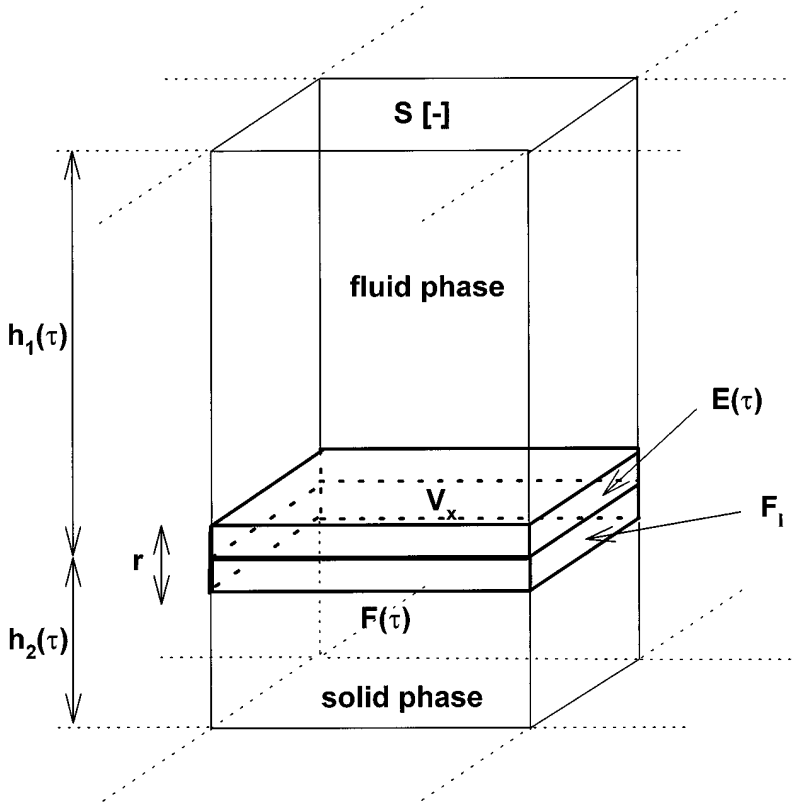

FIG. 1. **Geometrical relations at time τ in the subvolume of the reaction system for which the mathematical considerations are restricted.** The enzyme is applied in the bulk fluid phase above the reactive boundary layer and fibrin constitutes the solid phase under this layer. V_x, the examined subvolume of the reactive boundary layer; r, the depth of the reactive boundary layer; F_l, the number of substrate molecules in the boundary layer that are available for degradation in V_x; $h_1(\tau)$ and $h_2(\tau)$, the height of the fluid and solid phase, respectively, at time τ; $E(\tau)$ and $F(\tau)$, the total number of free enzyme molecules and intact fibrin monomers, respectively, in the examined subvolume at time τ.

$$\left(\frac{d[EF(\tau)/V_x]}{d\tau}\right)^{form} = k_1\left(\frac{E(\tau)}{S{\cdot}r}\right)^p \frac{F_l}{V_x} \quad |\cdot V_x \neq 0$$
$$\left(\frac{d[EF(\tau)]}{d\tau}\right)^{form} = k_1\left(\frac{E(\tau)}{S{\cdot}r}\right)^p F_l \qquad \text{(Eq. 2)}$$

The exponent of the enzyme concentration is introduced to express the changes in the dimensionality of the distribution of the kinetic energy of the enzyme molecules. 1) From the three-dimensional free movement in the bulk fluid phase, they bind to the surface of the fibrin fibers, suggesting two-dimensional movement (34, 35); and 2) on the other hand, internal diffusion or dissociation from the surface of the fiber increases the dimensionality of the reaction. These changes finally yield a non-integer value for the exponent, as evidenced by our measurements (see "Results"). The equation $E(\tau) = ((E_0 - EF(\tau))/(h_1(\tau)))\cdot r$, where E_0 [nmol/m^2] is the initial number of enzyme molecules per unit surface (calculated using the 10-fold concentration factor reported in Ref. 40) and $h_1(\tau)$ [m] is the height of the fluid phase at time τ, reflects the fact that the number of enzyme molecules is distributed between a free enzyme fraction and a fibrin-bound fraction. Applying the equation for area $S = 1$ and introducing $K_1' = k_1{\cdot}F_l$ [nmol$^{1-p}{\cdot}$m^{2-3p}/s], the following equation is derived.

$$\left(\frac{dEF(\tau)}{d\tau}\right)^{form} = K_1'\left(\frac{E_0 - EF(\tau)}{h_1(\tau)}\right)^p \qquad \text{(Eq. 3)}$$

The rate of EF dissociation to E and F (dissociation 1) is as follows.

$$(d[EF(\tau)/V_x]/d\tau)^{dis1} = -k_{-1}\frac{EF(\tau)}{V_x} \quad |\cdot V_x \neq 0$$
$$\left(\frac{dEF(\tau)}{d\tau}\right)^{dis1} = -k_{-1}EF(\tau) \qquad \text{(Eq. 4)}$$

The rate of EF degradation to E and P (dissociation 2) is as follows.

$$\left(\frac{dEF(\tau)/V_x}{d\tau}\right)^{dis2} = -k_2\left(\frac{EF(\tau)}{V_x}\right)^q \quad |\cdot V_x \neq 0$$
$$\left(\frac{dEF(\tau)}{d\tau}\right)^{dis2} = -k_2\cdot V_x^{1-q}\cdot EF(\tau)^q \qquad \text{(Eq. 5)}$$

In this case, the exponent of the EF was introduced in analogy to p as a mathematical experiment despite our expectation to gain a value of 1 (if the model assigns any value different from 1 to q, this will question the validity and the physical meaning of p in Equation 3). Considering that V_x is constant, K_2' is defined as follows.

$$k_2\cdot V_x^{1-q} = K_2' \quad [\text{nmol}^{1-q}\cdot\text{m}^{2q-2}/\text{s}] \qquad \text{(Eq. 6)}$$

$$\left(\frac{dEF(\tau)}{d\tau}\right)^{dis2} = -K_2'\cdot EF(\tau)^q \qquad \text{(Eq. 7)}$$

Thus, the overall rate of change of EF is as follows.

$$\frac{dEF(\tau)}{d\tau} = \left(\frac{dEF}{d\tau}\right)^{form} + \left(\frac{dEF}{d\tau}\right)^{dis1} + \left(\frac{dEF}{d\tau}\right)^{dis2} = K_1'\left(\frac{E_0 - EF(\tau)}{h_1(\tau)}\right)^p - k_{-1}\cdot EF(\tau) - K_2'EF(\tau)^q \qquad \text{(Eq. 8)}$$

Following an initial phase when the homogeneity of the reactive layer is established, the number of intact fibrin molecules per unit surface at time τ $F(\tau)$ is proportional to the height of the solid phase $h_2(\tau)$, thus there is a geometrical dependence,

$$h_1(\tau) = h_1^0 + h_2^0 - \frac{h_2^0 F(\tau)}{F_0} \qquad \text{(Eq. 9)}$$

where h_1^0 and h_2^0 stand for the height of the fluid and solid phase respectively at time 0, and F_0 is the initial number of fibrin molecules per unit surface.

Combining Equations 8 and 9 results in the following.

$$\frac{dEF(\tau)}{d\tau} = K_1'\left(\frac{E_0 - EF(\tau)}{h_1^0 + h_2^0 - \frac{h_2^0 F(\tau)}{F_0}}\right)^p - k_{-1}\cdot EF(\tau) - K_2'\cdot EF(\tau)^q \qquad \text{(Eq. 10)}$$

The overall rate of substrate consumption is as follows.

$$\frac{dF}{d\tau} = -\frac{dP}{d\tau} = -\left(-\frac{dEF}{d\tau}\right)^{dis2} = -K_2'EF^q$$
$$\frac{dF}{d\tau} = -K_2'\cdot EF^q \qquad \text{(Eq. 11)}$$

Exchange of the Independent Variable—In the experiments, we measured the time needed for the turbidity of the clot to decrease to a certain value, at which we have independent data for the amount of

undegraded fibrin (the residual non-cross-linked fibrin was determined with gel filtration as in Kolev *et al.* (23); the residual cross-linked fibrin was calculated from the data for protein concentration in the fluid phase determined with the method of Lowry *et al.* (47) and turbidimetric estimation of the volume of the fluid phase). Thus, the time represents the dependent variable that contains the experimental error. Consequently, it is justified to consider the momentary number of substrate molecules as an independent variable designated F [nmol/m^2].

$$\frac{dEF}{d\tau} = \frac{dEF}{dF}\frac{dF}{d\tau} \qquad \text{(Eq. 12)}$$

$$h_1^0 + h_2^0 = h^0 \qquad \text{(Eq. 13)}$$

Using Equations 10 and 11, Equation 12 is modified as follows:

$$\frac{dEF}{dF} = \frac{dEF/d\tau}{dF/d\tau} = 1 + \frac{k_{-1}}{K_2'}EF^{1-q} - \frac{K_1'}{K_2'EF^q}\left(\frac{(E_0 - EF)F_0}{F_0h^0 - h_2^0F}\right)^p \qquad \text{(Eq. 14)}$$

Summarizing the basic equations of the model follows.

$$\frac{dEF}{dF} = 1 + \frac{k_{-1}}{K_2'}EF^{1-q} - \frac{K_1'}{K_2'EF^q}\left(\frac{(E_0 - EF)F_0}{F_0h^0 - h_2^0F}\right)^p \qquad \text{(Eq. 15)}$$

From Equation 11, the exchange of the independent variable results in the following.

$$\frac{d\tau}{dF} = 1/\frac{dF}{d\tau} = \frac{1}{-K_2'EF^q} \qquad \text{(Eq. 16)}$$

At time $\tau = 0$, the following initial conditions are valid.

$$EF(F = F_0) = 0 \qquad \text{(Eq. 17)}$$

$$\tau(F = F_0) = 0 \qquad \text{(Eq. 18)}$$

For the system described so far, we formulate two mathematical problems: 1) to predict the time τ required for F_0 to decrease to a pre-determined value F_{kp} in a single experiment, if the parameters of the model (p, q, K_1', k_{-1}, K_2') are given; and 2) to determine the parameters of the model yielding minimal discrepancy between the values τ_{kp} predicted as in problem 1 and the values measured in a set of experiments for a group of enzymes with identical p and q exponents as introduced in Equations 3 and 5). Thus, we can confirm or rule out the necessity for such exponents. These problems are solved as described under "Appendix" with an original software written under Matlab® 4.0 with Simulink™ 1.2c (The MathWorks Inc., Natick, MA).

^{125}I-Labeled Proteins—Fibrinogen, plasmin, miniplasmin, and PMN-elastase were labeled by lactoperoxidase-catalyzed iodination, and ^{125}I-fibrin-coated tubes were prepared as described previously (29). The degradation of the fibrin monomer surface in the ^{125}I-fibrin-coated tubes was followed by measuring the radioactivity released into the fluid phase and by autoradiography after gel-electrophoresis of fluid phase samples. Penetration of ^{125}I-labeled and active site-blocked proteases into fibrin clots pre-formed in microplate wells was followed by measuring the residual radioactivity in the clot after removal of the fluid phase and rapid (5 s) washing of the fibrin surface.

RESULTS

Evaluation of the Model for Degradation of Fibrin Surface with Proteases—For determination of each set of kinetic parameters, at least 8 different concentrations of the protease in the range 0.02–2.4 μM are applied to the surface of preformed fibrin clots (cross-linked and non-cross-linked). All measurements are performed at least in triplicate, and the mean value and its standard error are used for the calculations as described in the mathematical procedures (see "Appendix"). The experimental approach is illustrated in Fig. 2 for the dissolution of cross-linked fibrin with plasmin. Identical experiments are carried out with all fibrinolytic enzymes on both cross-linked and non-cross-linked fibrin. Essentially identical parameter values are gained independently of the criterion used in the optimization procedure (absolute, relative, or general). For the sake of uniformity, only data from procedures with the relative criterion are reported in Tables I and II (in this case the relative square error of the function can be used to evaluate the reliability of the parameter values). The predictive value of the model can be estimated on the basis of the comparison of the empirical data with the corresponding calculated values. An example for the good agreement of theoretical and empirical data is provided in Fig. 3 for the dissolution of non-cross-linked fibrin with miniplasmin. In addition, the model predicts the absolute surface concentration of the enzyme-fibrin complexes. Its value does not exceed 10% of the respective initial enzyme concentration. Even when the optimization procedure does not use the steady-state assumption (first and second method under "Appendix"), this value does not vary by more than 5% in the course of the studied reactions following the initial negligibly short pre-steady-state period. The identity of the results gained with the three computation methods supports the validity of the steady-state assumption for the examined system and justifies its usage in the computation procedure (computation time is at least 100-fold shorter when working with this assumption). If the optimization procedure is allowed to freely vary, the values of the exponents p and q in Equations 3 and 5, it consistently assigns a value of 1 to q and a non-integer value to p. Thus, the model does not tolerate arbitrarily introduced parameters (there is no reason to suggest a value different from 1 for the order of the $EF \rightarrow E + P$ reaction, whereas sound arguments can be brought in favor of the non-integer value of p). For $q = 1$ K_2' is equal to k_2 (Equation 6). Since we interpret the values of p as a result of changes in the dimensionality of the $E + F_l \rightarrow EF$ reaction, in separate experiments, we evaluate indirectly the relative contribution of the attacks from the bulk phase (three-dimensional reaction) and from lateral migration (two-dimensional reaction) to the rate of EF complex formation. In the initial period after the application of the enzyme solution over the fibrin surface, obviously, the three-dimensional events dominate. In accordance with this, if the enzyme solution is replaced with buffer within 2 min after the application and

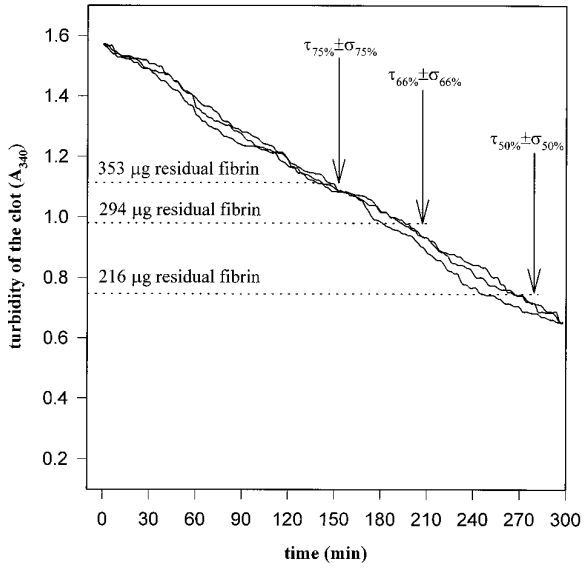

FIG. 2. **Changes of turbidity in the course of cross-linked fibrin dissolution.** Cross-linked fibrin (400 μg) was prepared as described under "Experimental Procedures" in a buffer containing 75 mM NaCl. Cross-linking was complete in 16 h, and, thereafter, 100 μl of 160 nM plasmin is applied to the fibrin surface. The curves represent the change of turbidity (A_{340}) following the application of the enzyme. At the indicated three different levels of the clot turbidity, the amount of residual fibrin is independently determined by measuring the concentration of protein content in the fluid phase. As shown, at least three parallel measurements are performed for each separate enzyme concentration, and their mean value as well as standard error are evaluated in a single calculation procedure for all eight different enzyme concentrations.

TABLE I

Kinetic parameters for digestion of non-cross-linked fibrin

The values are calculated as described under "Experimental Procedures" on the basis of data gained in the experimental design illustrated in Fig. 2. For these measurements, the fibrin substrate is polymerized at 75 mM NaCl.

Enzyme	$k_2 \times 10^2$	$K_1' = k_1 \cdot F_l$	k_{-1}	$k_2 \cdot K_1'/(k_2 + k_{-1}) \times 10^2$	p	Relative square error of the function
	s^{-1}	$m^{3p-2} \cdot nmol^{1-p} \cdot s^{-1}$	s^{-1}	$m^{3p-2} \cdot nmol^{1-p} \cdot s^{-1}$		%
Plasmin	3.87	86.4	57.6	5.80	0.34	9.8
Miniplasmin	3.93	83.9	81.8	4.03	0.32	8.7
Microplasmin	0.81	44.8	19.7	1.84	0.31	15.2
PMN-elastase	0.58	83.0	55.7	0.86	0.27	5.3
Trypsin	3.62	93.2	96.7	2.88	0.43	23.2

TABLE II

Kinetic parameters for digestion of cross-linked fibrin

The values are calculated as described under "Experimental Procedures" on the basis of data gained in the experimental design illustrated in Fig. 2. For these measurements, the fibrin substrate is polymerized at 75 mM NaCl.

Enzyme	$k_2 \times 10^2$	$K_1' = k_1 \cdot F_l$	k_{-1}	$k_2 \cdot K_1'/(k_2 + k_{-1}) \times 10^2$	p	Relative square error of the function
	s^{-1}	$m^{3p-2} \cdot nmol^{1-p} \cdot s^{-1}$	s^{-1}	$m^{3p-2} \cdot nmol^{1-p} \cdot s^{-1}$		%
Plasmin	8.99	16.0	85.9	1.67	0.25	9.3
Miniplasmin	16.32	16.9	67.3	4.08	0.22	21.0
Microplasmin	0.73	24.6	13.7	1.31	0.30	10.0
PMN-elastase	0.65	14.9	55.7	0.17	0.41	9.7
Trypsin	3.34	42.0	96.5	1.45	0.34	13.1

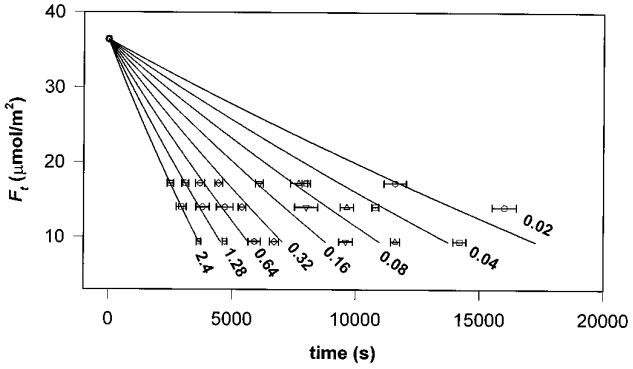

FIG. 3. **Rate of fibrin consumption in the course of the dissolution process with miniplasmin.** Non-cross-linked fibrin was prepared as described under "Experimental Procedures" in a buffer containing 75 mM NaCl. Miniplasmin is applied to the surface of the clot in a volume of 100 μl at the concentrations (in μM) indicated at the end of each line by the respective *symbol*. The time to reach three pre-determined fibrin levels is measured, as illustrated in Fig. 2. The *symbols* represent the measured time values with their standard deviations, whereas the values predicted by the model are shown by *lines*.

subsequently the clot is washed 3 times with an enzyme-free buffer (each volume of the washing buffer is left for 2 min over the fibrin), the dissolution process is completely stopped. If the fibrin surface is washed 3 or 5 times in the same way with a protease-free buffer later than 2 min following the application of the enzyme, the rate of A_{340}-change decreases 3-fold, but no complete inhibition of fibrinolysis can be achieved. This residual fibrinolytic activity can be attributed to the migration of the enzyme molecules along the fibrin fibers. The data of this functional assay are confirmed by the rate of penetration of ^{125}I-labeled and active-site blocked enzymes into fibrin clots. When the incorporation of radioactivity from solutions of ^{125}I-plasmin-PMSF, ^{125}I-miniplasmin-PMSF or ^{125}I-PMN-elastase-PMSF into fibrin is measured, in the first minute after the application of the enzyme over the fibrin surface, a burst in the radioactivity of the clot is observed, whereas in the next 5 h, a linear, but 100-fold slower, increase in the clot-bound radioactivity can be detected (not shown). The dissociation of the clot-bound proteases is relatively slow compared with the binding. If, following 1-min binding, the clot is rapidly (10 s) washed three times with enzyme-free buffer and the last volume of washing buffer is left over the clot, 70% of the enzyme-related radioactivity is retained in the clot 1 h later. If plasmin is applied to a fibrin monomer surface, 6AH (which interferes with the interaction between the kringle domains of plasmin and lysine residues in fibrin) inhibits its fibrinolytic activity at concentrations in the micromolar range when it has been pre-incubated with the enzyme, whereas an order of magnitude higher concentration of 6AH is needed for a similar effect when the 6AH is added following the enzyme binding to the fibrin (Fig. 4, *A* and *C*). This, together with the time-course of the inhibition in the second case (30 min are needed to reach the full inhibiting effect, Fig. 4*C*, *inset*) suggests high processivity for the plasmin molecule. Once bound to the substrate, the enzyme dissociates relatively rarely into the bulk phase where 6AH blocks its lysine-binding sites. Blocking of the single lysine-binding site of miniplasmin with 6AH (Fig. 4*B*) has a less expressed effect on the fibrinolytic activity of this protease compared with plasmin, and 60 min are needed for the maximal inhibition when 6AH is added after the miniplasmin binding to fibrin (Fig. 4*D*, *inset*). The latter fact emphasizes the importance of the fifth kringle in the processive properties of the enzyme.

Effect of Fibrin Network Structure on the Catalytic Properties of Plasmin—Fibrin gel with varying fiber diameter and porosity was prepared by clotting fibrinogen in solutions containing different concentrations of Cl^-, which determines the polymerization pattern (46). For each type of fibrin gel, plasmin (at eight different concentrations in the range 0.05–1.2 μM) is applied to the surface of the clot in a solution yielding a final concentration of 150 mM NaCl in the total volume of the clot and fluid phase. Using the approach described under "Experimental Procedures," the kinetic parameters of Equations 3–5 and 7. can be determined for the dissolution of the different fibrin clots by plasmin. In parallel with the increase of the Cl^- concentration at polymerization, the apparent k_2 increases, whereas the exponent of the enzyme concentration p decreases (Fig. 5). The parameters for the formation ($K_1' = k_1 \cdot F_l$) and dissociation (k_{-1}) of the enzyme-fibrin complex do not change significantly ($K_1' = 105.2 \pm 8.8$ $m^{3p-2} \cdot nmol^{1-p}/s$, $k_{-1} = 54.1 \pm 4.1$ s^{-1}). Thus, the catalytic efficiency ratio ($k_2 \cdot K_1'/(k_2 + k_{-1})$) follows the tendency of k_2 (Fig. 5.).

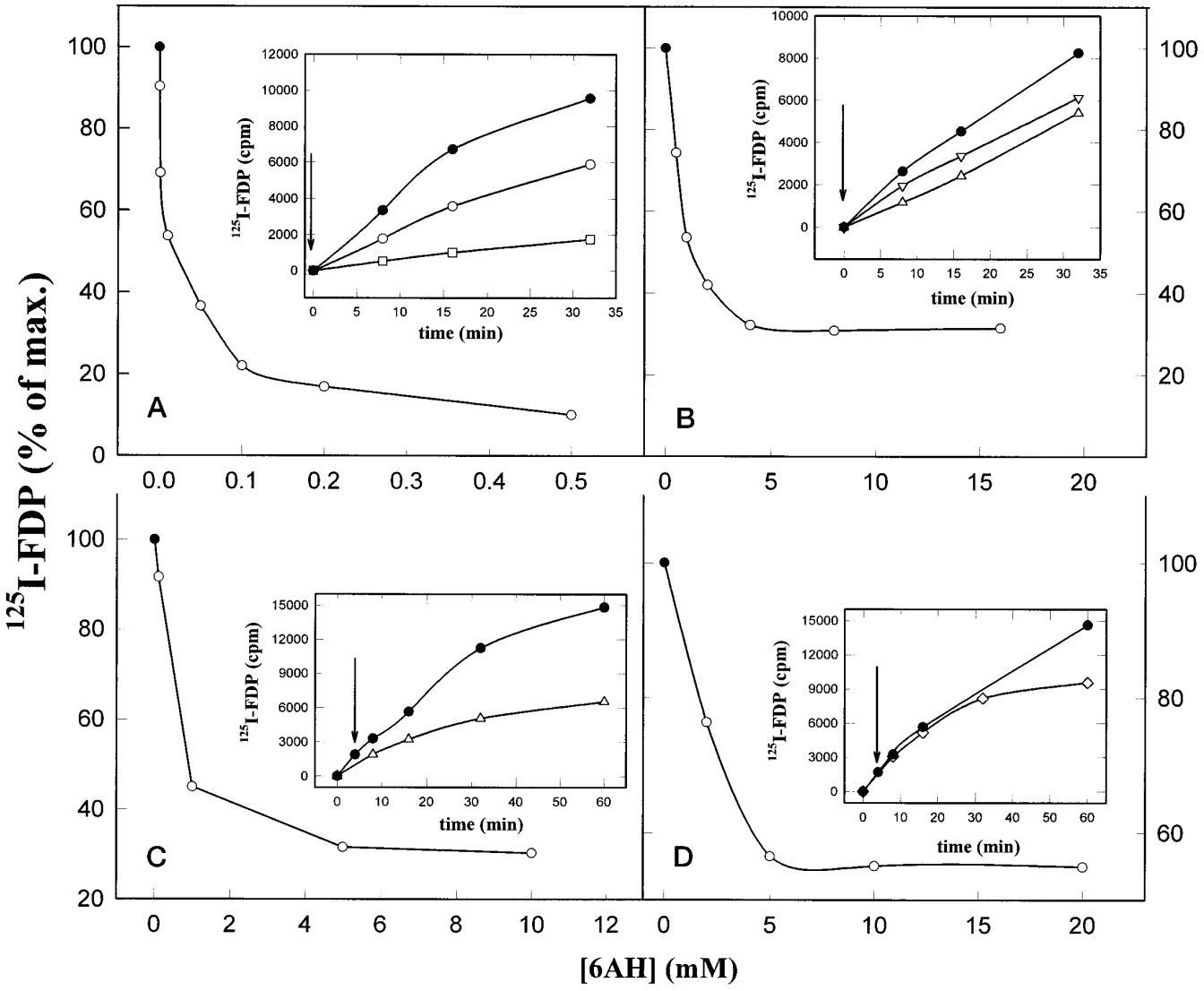

FIG. 4. **Effect of 6-aminohexanoate on the rate of degradation of fibrin monomers with plasmin and miniplasmin.** ^{125}I-fibrin-coated tubes are incubated with plasmin at 1 nM concentration (*A* and *C*) or miniplasmin at 4 nM concentration (*B* and *D*). 6AH is added at the indicated concentrations either simultaneously with the enzyme (*A* and *B*) or after 4 min of pre-incubation of the enzyme on the fibrin-monomer surface (*C* and *D*). The radioactivity of the released degradation products is measured at 16 (*A* and *B*), 32 (*C*), or 60 min (*D*). Results are expressed in percent of the radioactivity released in the absence of 6AH. *Insets*, time-course of fibrin degradation in the absence (*filled symbols*) or presence (*empty symbols*) of 6AH added at the time indicated by *arrows*. Concentrations of 6AH are 10 μM (○), 200 μM (□), 500 μM (▽), 1 mM (△), and 5 mM (◇). *^{125}I-FDP*, ^{125}I-labeled fibrin degradation products.

Quantitative Comparison of Fibrin Surface Degradation with Different Proteases—Each of the studied proteases is applied to the surface of a pre-formed fibrin clot at eight different concentrations and from the turbidimetric data the kinetic parameters (p, k_2, K_1', k_{-1}) introduced in Equations 3–5 and 7 are calculated for each separate enzyme regarded as a "group" in the sense of problem 2. The results for non-cross-linked fibrin are summarized in Table I and for cross-linked fibrin in Table II. For estimation of the role of polymerization in the dissolution process, the degradation of ^{125}I-labeled fibrin monomer surface is also followed (Fig. 6). The *inset* shows that digestion of the labeled fibrin yields products that are essentially identical with those of native, unlabeled polymerized fibrin (23), suggesting that the labeling technique does not modify the region of the fibrin molecule degraded by the proteases.

DISCUSSION

With the introduced approach, several discrete steps in the process of fibrin dissolution with extrinsic proteases can be characterized. The detachment of water-soluble degradation products from the fibrin fibers that is detected as dissolution of the clot or change in its turbidity is rate-limited by the proteolytic reaction that is characterized by the apparent k_2 constant. This constant is apparent because more than one peptide bond is cleaved for the release of a single soluble product (thus this value is a global integrated constant), and its value depends on the actual accumulation of enzyme in the reactive boundary layer (in all calculations, we assume an average 10-fold accumulation compared with the fluid phase as reported in Sakharov and Rijken (40)). We do not correct the value of k_2 for the number of cleaved bonds because, in this way, the constant is more suitable for comparison of different proteases in their efficiency in the global process of fibrin dissolution. The soundness of the approach is supported by the data gained for clot-embedded plasmin. We earlier found a k_2 of 6×10^{-2} s^{-1} for 2.5 g/l fibrin at 150 mM NaCl and 3 mM $CaCl_2$ (23), whereas our present result shown in Fig. 5 is 8.6×10^{-2} s^{-1}. Our findings are in good agreement with the single available report in the literature (39). Under conditions similar to ours (for 3 g/l fibrin

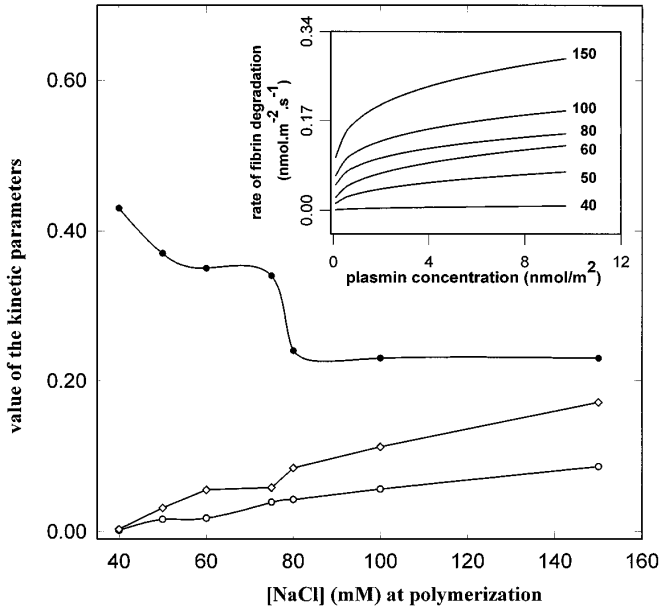

FIG. 5. **Effect of the structure of non-cross-linked fibrin polymerized at different Cl^- concentrations on the kinetic parameters for fibrin dissolution with plasmin.** The parameters of the kinetic model p (●, exponent for the enzyme concentration) and k_{cat} (○, s^{-1}) are presented. The ratio of the kinetic constants $k_2 \cdot K_1'/(k_2 + k_{-1})$ (◇) is calculated for evaluation of the catalytic efficiency. *Inset*, estimated rate of fibrin dissolution with plasmin applied to the surface of the substrate polymerized at different Cl^- concentrations. Representative rates of fibrin dissolution are calculated for various E_0 from Equation 7 applying an average value for EF gained from Equation 10 at $F_\tau = (F_0 + F_{kp})/2$ and using the parameters from this figure (the numbers at the end of the *curves* indicate the concentration of NaCl in mM at which fibrin is polymerized).

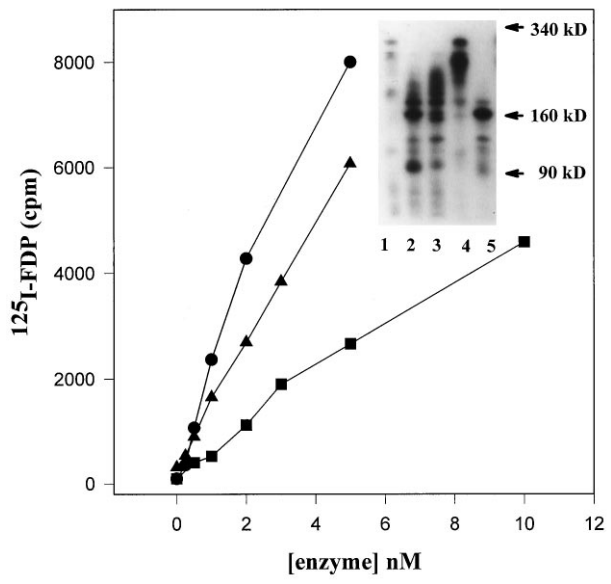

FIG. 6. **Degradation of fibrin monomers with plasmin, miniplasmin, and PMN-elastase.** Plasmin (●), miniplasmin (■), or PMN-elastase (▲) is applied to a surface of fibrin monomers in ^{125}I-fibrin-coated tubes, and after 8 min, ^{125}I-labeled fibrin degradation products (^{125}*I-FDP*) release is measured. Radioactivity release is linear for at least 16 min (not shown). *Inset*, autoradiograph of 7.5% polyacrylamide gel after electrophoresis of ^{125}I-labeled products released by 10 g/l bovine serum albumin (*lane 1*), 5 nM plasmin (*lane 2*), 10 nM miniplasmin (*lane 3*), 5 nM PMN-elastase (*lane 4*), or 10 nM miniplasmin and 5 nM PMN-elastase together (*lane 5*).

prepared at 100 mM NaCl and 5 mM $CaCl_2$) a k_2 of 5 s^{-1} is found for plasmin if a solubilization factor (number of lyzed bonds per solubilized monomer) of 10 is used (with the same assumption and ignoring the accumulation of enzyme in the boundary layer, our result from Fig. 5 should be 5.61 s^{-1}). Our data for the parameters of enzyme-fibrin complex formation ($k_1 \cdot F_l$ and k_{-1}) are remarkably constant, independent of the changes in the structure of the fibrin substrate as the Cl^- concentration at polymerization is varied. This justifies the application of a constant accumulation ratio for the enzyme in the boundary reactive layer, which was mentioned as a second factor for the ostensibility of k_2. Thus, the increase of k_2, observed as the substrate polymer fibers become thinner and their branching points more frequent at higher Cl^- concentration (Fig. 5), can be interpreted as a consequence either of a more suitable exposure of the proteolysis-susceptible bonds or of a reduction in the number of bonds that should be broken for the solubilization of a single monomer. Another parameter that changes markedly with the alteration of the substrate structure is the exponent p of the enzyme concentration in the kinetic equation (Equation 14). Higher values of this parameter suggest preservation of the kinetic energy of the enzyme molecule for effective attacks, whereas low values reflect "energy loss" for dissociation from the fiber surface and diffusion among the fibers. If this interpretation is applied to the values of p shown in Fig. 5., a conclusion can be drawn that the coarse fibrin polymerized at low Cl^- concentration channels the enzyme within the thick fibers and reduces the dimensionality of its movement, whereas in the thin fibrin formed at higher Cl^- concentration, detachment from the fiber and migration among the fibers occurs more frequently, resulting in increase in the dimensionality of the enzyme movement and reduction of p. The 30 and 60 min delays in the maximal effect of 6AH on the fibrinolytic activity of plasmin and miniplasmin (Fig. 4.) also support the idea of enzyme channeling along the fibrin surface. Due to the non-integer value of p, the catalytic efficiency of plasmin on the different fibrin substrates cannot be evaluated simply on the basis of the ratio $k_2 \cdot K'_1/(k_2 + k_{-1})$, but the effect of p should also be considered. From the simulated curves in Fig. 5, *inset*, a definite conclusion can be drawn that the thinner and extensively branched fibers of fibrin formed at higher Cl^- concentrations are more efficiently dissolved by plasmin at all enzyme concentrations. Similar changes of fibrin structure can be induced by variations of fibrinogen and thrombin concentrations (4, 5), which *in vivo* can yield fibrin of different susceptibility to plasmin.

When the kinetic data for the three proteases with identical catalytic domain (plasmin, miniplasmin, and microplasmin) are compared, important conclusions about the structure-function relationship in the molecule of plasmin can be drawn. Similarly to fibrinogen as a substrate (21, 22), the kinetic parameters of plasmin and miniplasmin on non-cross-linked fibrin are essentially identical. The only exception is k_{-1}, which is markedly higher for miniplasmin (Table I; our model discriminates the association and dissociation constants for the formation of enzyme-substrate complex based on the different order of the two reactions). This suggests that the first four kringle domains are needed to retain the enzyme in the enzyme-fibrin complex. The fifth kringle seems to contribute to the maintenance of the appropriate conformation of the catalytic domain and to the affinity of the enzyme to the proteolysis susceptible sites; the absence of $kringle_5$ in microplasmin is related to a markedly lower k_2 and association constant compared with plasmin and miniplasmin. Trypsin, a protease of similar primary specificity to plasmin (it cleaves peptide bonds at basic amino acids), shows the same k_2 as plasmin, but its affinity to fibrin estimated on the basis of the ratio of the association and dissociation constants for the enzyme-substrate complex is markedly lower compared with plasmin and

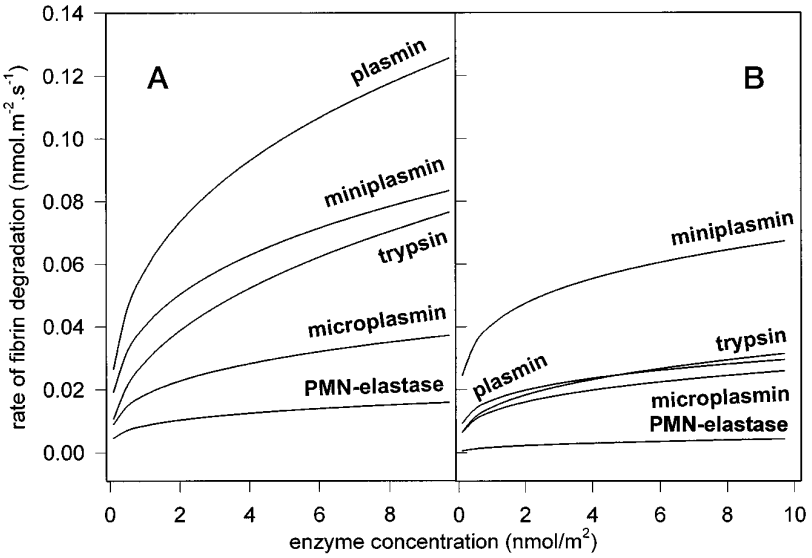

FIG. 7. **Estimated rate of fibrin dissolution with enzymes applied to the surface of the polymer.** Representative rates of fibrin dissolution are calculated for various E_0 from Equation 7, applying an average value for EF gained from Equation 10 at $F_\tau = (F_0 + F_{kp})/2$ and using the parameters for non-cross-linked fibrin from Table I (*A*) and cross-linked fibrin from Table II (*B*).

even microplasmin. The latter suggests that, in addition to the kringle domains, the structure of the catalytic domain in plasmin also contributes to its specificity for fibrin. PMN-elastase, another protease of potential relevance to fibrinolysis *in vivo*, demonstrates similar affinity to fibrin as plasmin, but its catalytic constant is almost an order of magnitude lower. Due to the different values of the exponent p for the enzyme concentration in Equation 14, comparison of the catalytic efficiency of the separate proteases is possible only on the basis of the simulated curves in Fig. 7*A*, which indicates that among the physiologically relevant enzymes the most efficient in the dissolution of non-cross-linked fibrin is plasmin followed by miniplasmin and PMN-elastase. Since on fibrin monomers the proteolytic activity of PMN-elastase is similar to that of plasmin and better than that of miniplasmin (Fig. 6.), the estimated low efficiency of PMN-elastase in polymerized fibrin dissolution can be explained by the relatively higher number of bonds that should be broken for the solubilization of a single monomer or alternatively by masking of the elastase-susceptible peptide bonds in the polymer. The latter possibility, however, is less probable if the identical degradation products from fibrin monomers and clots are considered (Fig. 6, *inset* and Ref. 23). The relative order of efficiency for dissolution of non-cross-linked fibrin clots with extrinsic proteases is the same as that established for the clot-embedded enzymes (23).

An important aspect of fibrinolysis *in vivo* is the influence of cross-linking by factor XIIIa on the dissolution properties of fibrin. Our results reveal new details of the well documented resistance of the cross-linked fibrin to proteolysis (7–12). Surprisingly, the k_2 on cross-linked fibrin for plasmin and miniplasmin is 2–4-fold higher than on non-cross-linked fibrin (this parameter is only slightly modified for the other three studied enzymes) (Table II). The general tendency for significant reduction of the association rate constant K_1', however, explains the relative proteolytic resistance of the cross-linked fibrin. Cross-linking probably renders the fibrin monomers a conformation to which the proteases show low affinity, but the rate of the separate proteolytic steps is either not influenced (microplasmin, PMN-elastase, trypsin) or even enhanced (plasmin, miniplasmin). Using the ratio of the kinetic parameters and the value of the exponent for the enzyme concentration p (Table II), the proteolytic activity of the separate proteases on cross-linked fibrin can be compared (Fig. 7*B*). The relative order of catalytic efficiency of the physiologically relevant fibrinolytic proteases is different on cross-linked fibrin surface; the most effective is miniplasmin, followed by plasmin and PMN-elastase. Thus, PMN-elastase, despite its relatively low direct fibrinolytic activity, can contribute to the dissolution of fibrin through the generation of miniplasmin, the most efficient protease on stabilized fibrin.

Acknowledgment—We are grateful to Ida Horváth, Györgyi Oravecz, Antoaneta Krasteva, and Ágnes Himer for technical assistance.

APPENDIX

The numerical solutions of the basic mathematical problems are as follows.

Problem No. 1

The parameters of each experiment are *cons*; h^0; h_1^0; E_0; F_0; K_1'; K_2'; k_{-1}; p; q; and F_{kp}. F_{kp} [nmol/m^2] is the surface concentration of intact fibrin monomers at the examined levels of clot turbidity determined by gel-filtration chromatography for non-cross-linked fibrin or with protein determination for cross-linked fibrin. The *cons* is a flag indicating the availability of previously calculated parameters from the same experiment for $F_{kp}^* > F_{kp}$ ($cons = 1$) or their absence ($cons = 0$). The asterisk always designates calculated parameters from a previous level, if $cons = 1$. The value of τ_{kp} should be calculated. Three different methods are applied for the solution of the problem.

First Method Is System of Differential Equations—Equations 15 and 16 are solved as a system of two differential equations with initial conditions Equations 17 and 18 for the interval $F = [F_0;F_{kp}]$. Equations 15 and 16 are integrated from F_0 to F_{kp} at $cons = 0$ and from F_{kp*} to F_{kp} at $cons = 1$. At $cons = 0$, the real initial conditions (Equations 17 and 18) are singular and cannot be used as a start point for the solution. The modified boundary conditions,

$$\tau(F_0) = 0$$

$$EF(F_0) = \frac{EF_r(F_0)}{1000} \qquad \text{(Eq. 19)}$$

where $EF_r(F_0)$ is the equilibrium concentration of the complex at the initial moment. The latter is gained from the solution of the non-linear equation $dEF/d\tau = 0$ (see Equation 10) for EF at $F = F_0$. At $cons = 1$, the initial conditions are as follows.

$$\tau(F_{kp}^*) = \tau_{kp}^*$$

$$EF(F_{kp}^*) = EF_{kp}^* \qquad \text{(Eq. 20)}$$

Second Method Is Differential Equation for EF—In this procedure, we regard all the measurements with the same enzyme at a given E_0 from F_0 to the different F_{kp}s as separate experiments belonging to the same family. In each family, the experiment with the highest F_{kp} has *cons* = 0, whereas all others have *cons* = 1. In the system of differential Equations 15 and 16, Equation 15 can be solved separately because the right side of the equation does not depend on τ. Solving Equation 15 in the range $[F_0;(F_{kp})_{\min}]$ (using the modified boundary condition for *EF* as in the first method), a table for *EF-F* can be derived that contains $n + 1$ pairs of values for $EF_i - F_i$ ($i = 0, 1, 2, \ldots, n$). In each of the n intervals $[F_i;F_{i+1}]$, the function $EF(\tau)$ can be replaced with the linear function,

$$\begin{aligned} EF &= a_i \cdot F + b_i \quad \text{where} \\ a_i &= \frac{EF_{i+1} - EF_i}{F_{i+1} - F_i} \\ b_i &= EF_i - a_i F_i \end{aligned} \qquad \text{(Eq. 21)}$$

Thereafter Equation 16 is integrated in the interval $[F;(F_{i+1})_{\min}]$ and replacing Equation 21 in Equation 16 is as follows.

$$\tau_{i+1} = \tau_i - \frac{1}{K_2'} \int_{F_i}^{F_{i+1}} \frac{dF}{(b_i + a_i \cdot F)^q} = \tau_i - \frac{1}{K_2' \cdot a_i} \int_{F_i}^{F_{i+1}} \frac{d(a_i \cdot F + b_i)}{(b_i + a_i \cdot F)^q} \qquad \text{(Eq. 22)}$$

The result of Equation 22 depends on q;
for $q \neq 1$

$$\tau_{i+1} = \tau_i - \frac{1}{K_2' \cdot a_i} \cdot \frac{(a \cdot F + b)^{-q+1}}{-q+1} \Big|_{F_i}^{F_{i+1}} =$$

$$\tau_i - \frac{1}{K_2' a_i} \cdot \frac{(a_i F_{i+1} + b_i)^{-q+1} - (a_i F_i + b_i)^{-q+1}}{-q+1} \qquad \text{(Eq. 23)}$$

for $q = 1$

$$\tau_{i+1} = \tau_i - \frac{1}{K_2' \cdot a_i} \ln(a_i \cdot F + b_i) \Big|_{F_i}^{F_{i+1}} = \tau_i - \frac{1}{K_2' \cdot a_i} \ln \frac{a_i \cdot F_{i+1} + b_i}{a_i \cdot F_i + b_i} \qquad \text{(Eq. 24)}$$

For each experiment, the newly calculated value is added to the table; using linear interpolation, the table is further extended and all data after F_{kp} are deleted. For each experiment, τ_{kp} is calculated after multiple applications of Equations 23 or 24.

$$\tau_{kp} = \int_{F_0}^{F_{kp}} \frac{1}{-K_2' \cdot EF^q} dF = \sum_{i=0}^{n'} - \frac{1}{K_2'} \int_{F_i}^{F_{i+1}} \frac{dF}{EF^q} \qquad \text{(Eq. 25)}$$

In Equation 25, n' is the number of intervals from the table between F_0 and F_{kp}.

Third Method Is Non-linear Equation for EF—With this method, we assume that the rate of formation of *EF* is equal to the rate of its degradation at each moment of time (this is not equivalent to the assumption that the amount of *EF* does not change in the course of the reaction). The range $[F_0;(F_{kp})_{\min}]$ is divided by $n + 1$ points, $F_0,F_1,F_2,F_3,\ldots F_n = (F_{kp})_{\min}$.

For each F_i value, a value for EF_i is calculated from $dEF/dt = 0$ using Equation 10. Thus, an $EF_i - F_i$ table is composed that contains $n + 1$ pairs $EF_i - F_i$. The last step is integration according to Equation 25 as under "Second Method."

Problem No. 2

A group of "e" enzymes with common p and q exponents (Equations 3 and 5) is considered ($i = 1, 2 \ldots e$), where enzyme i is characterized by parameters p, q, K'^i_1, K'^i_2, k^i_{-1}. For each enzyme n_i, different experiments are available ($j = 1, 2 \ldots n_i$). The experiment j with the enzyme i is repeated $m_{ij} > 1$ times ($3 \leq m_{ij} \leq 6$), and the following experimental times are measured $\tau^1_{ij}, \tau^2_{ij}, \ldots \tau^k_{ij}, \ldots \tau^{mij}_{ij}$.Let

$$\begin{aligned} \vec{K}'_1 &= (K'^1_1, K'^2_1, \ldots, K'^e_1)^t \\ \vec{K}'_2 &= (K'^1_2, K'^2_2, \ldots, K'^e_2)^t, \\ \vec{k}_{-1} &= (k'^1_{-1}, k'^2_{-1}, \ldots, k'^e_{-1})^t \end{aligned} \qquad \text{(Eq. 26)}$$

where t is a sign for transposition.

The parameters $p,q,\vec{K}'_2,\vec{K}'_1,\vec{k}_{-1}$ should be determined so that the calculated τ optimally approaches the experimental one. The mean τ^{ex}_{ij} and its standard error σ_{ij} are determined as follows.

$$\tau^{ex}_{ij} = \sum_{k=1}^{m_{ij}} \tau^k_{ij} / m_{ij} \qquad \text{(Eq. 27)}$$

$$\sigma_{ij} = \sqrt{\frac{\sum_{k=1}^{m_{ij}} (\tau^k_{ij} - \tau^{ex}_{ij})^2}{m_{ij} - 1}} \qquad \text{(Eq. 28)}$$

If τ^{kp}_{ij} is the calculated time from the model with parameters corresponding to the j-th experiment with the i-th enzyme, the following criteria are used for the identification of the parameters.

Absolute criterion

$$\chi^2_{abs}(p,q,\vec{K}'_1,\vec{K}'_2,\vec{k}_{-1}) = \sqrt{\frac{1}{\alpha^2\beta} \sum_{i=1}^{e} \sum_{j=1}^{n_i} \left[\frac{\tau^{kp}_{ij}(p,q,K'^i_1,K'^i_2,k^i_{-1}) - \tau^{ex}_{ij}}{\sigma_{ij}} \right]^2} \quad [-] \qquad \text{(Eq. 29)}$$

$$\chi^2_{abs}(p,q,\vec{K}'_1,\vec{K}'_2,\vec{k}_{-1}) = \frac{1}{60} \cdot \sqrt{\frac{1}{\beta} \sum_{i=1}^{e} \sum_{j=1}^{n_i} \left[\frac{\tau^{kp}_{ij}(p,q,K'^i_1,K'^i_2,k^i_{-1}) - \tau^{ex}_{ij}}{\sigma_{ij}} \right]^2} \quad [\text{min}] \qquad \text{(Eq. 30)}$$

Relative criterion

$$\chi^2_{rel}(p,q,\vec{K}'_1,\vec{K}'_2,\vec{k}_{-1}) = \sqrt{\frac{1}{\beta} \sum_{i=1}^{e} \sum_{j=1}^{n_i} \left[\frac{\tau^{kp}_{ij}(p,q,K'^i_1,K'^i_2,k^i_{-1}) - \tau^{ex}_{ij}}{\sigma_{ij} \cdot \tau^{ex}_{ij}} \right]^2} \quad [-] \qquad \text{(Eq. 31)}$$

$$\chi^2_{rel}(p,q,\vec{K}'_1,\vec{K}'_2,\vec{k}_{-1}) = 100 \cdot \sqrt{\frac{1}{\beta} \sum_{i=1}^{e} \sum_{j=1}^{n_i} \left[\frac{\tau^{kp}_{ij}(p,q,K'^i_1,K'^i_2,k^i_{-1}) - \tau^{ex}_{ij}}{\sigma_{ij} \cdot \tau^{ex}_{ij}} \right]^2} \quad [\%] \qquad \text{(Eq. 32)}$$

General criterion

$$\chi^2_{com}(p,q,\vec{K}'_1,\vec{K}'_2,\vec{k}_{-1}) = \sqrt{\frac{1}{\alpha\beta} \sum_{i=1}^{e} \sum_{j=1}^{n_i} \left[\frac{\tau^{kp}_{ij}(p,q,K'^i_1,K'^i_2,k^i_{-1}) - \tau^{ex}_{ij}}{\sigma_{ij} \cdot \sqrt{\tau^{ex}_{ij}}} \right]^2} \quad [-] \qquad \text{(Eq. 33)}$$

$$\chi^2_{com}(p,q,\vec{K}'_1,\vec{K}'_2,\vec{k}_{-1}) = \frac{1}{60 \cdot \beta} \sum_{i=1}^{e} \sum_{j=1}^{n_i} \left[\frac{\tau^{kp}_{ij}(p,q,K'^i_1,K'^i_2,k^i_{-1}) - \tau^{ex}_{ij}}{\sigma_{ij} \cdot \sqrt{\tau^{ex}_{ij}}} \right]^2 \quad [\text{min}] \qquad \text{(Eq. 34)}$$

In the equations above, α and β are weighing coefficients introduced to make the χ^2 dimensionless with a value usually within the range (0;1). These coefficients are defined as follows.

$$\alpha = \frac{\sum_{i=1}^{e} \sum_{j=1}^{n_i} \tau^{ex}_{ij}}{\sum_{i=1}^{e} n_i} \qquad \beta = \sum_{i=1}^{e} \sum_{j=1}^{n_i} \frac{1}{\sigma^2_{ij}} \qquad \text{(Eq. 35)}$$

The optimized parameters are determined after minimization of a selected criterion in the following situations,

$$\chi^2(p,q,\vec{K}'_1,\vec{K}'_2,\vec{k}_{-1}) \quad \text{(Eq. 36)}$$

with free variations of all parameters,

$$\chi^2(p,\vec{K}'_1,\vec{K}'_2,\vec{k}_{-1}) \quad \text{(Eq. 37)}$$

with fixed q (usually $q = 1$),

$$\chi^2(\vec{K}'_1,\vec{K}'_2,\vec{k}_{-1}) \quad \text{(Eq. 38)}$$

with fixed p and q (usually $p = 1$ and $q = 1$).

The optimization procedure uses Equations 29, 31, and 33, but the results are presented according to Equations 30, 32, and 34, which show the errors with their dimensions.

REFERENCES

1. Hantgan, R. R., Francis, C. W., and Marder, V. J. (1994) in *Hemostasis and Thrombosis: Basic Principles and Clinical Practice* (Colman, R. W., Hirsh, J., Marder, V. J., and Salzman, E. W., eds) pp. 277–300, J. B. Lippincott Co., Philadelphia, PA
2. Baradet, T. C., Haselgrove, J. C., and Weisel, J. W. (1995) *Biophys. J.* **68,** 1551–1560
3. Carr, M. E. Jr., Shen, L. L., and Hermans, J. (1977) *Biopolymers* **16,** 1–15
4. Carr, M. E., Jr., Gabriel, D. A., and McDonagh, J. (1986) *Biochem. J.* **239,** 513–516
5. Blombäck, B., Carlsson, K., Hessel, B., Liljeborg, A., Procyk, R., and Åslund, N. (1989) *Biochim. Biophys. Acta* **997,** 96–110
6. Muszbek, L., and Laki, K. (1984) in *The Thrombin* (Machovich, R., ed) pp. 83–102, CRC Press, Boca Raton, FL
7. Lorand, J. B., Pilkington, T. R., and Lorand, L. (1966) *Nature* **210,** 1273–1274
8. McDonagh, R. P., McDonagh, J., and Duckert, F. (1971) *Br. J. Haematol.* **21,** 323–332
9. Schwartz, M. L., Pizzo, S. V., Hill, R. L., and McKee, P. A. (1973) *J. Biol. Chem.* **248,** 1395–1407
10. Francis, C. W., and Marder, V. J. (1988) *Blood* **71,** 1361–1365
11. Francis, C. W., and Marder, V. J. (1986) *J. Lab. Clin. Med.* **107,** 342–352
12. Carmassi, F., Cardinali, M., Bianchi, R., and Chung, S. I. (1990) *Fibrinolysis* **3,** 45–51
13. Bachmann, F. (1994) in *Hemostasis and Thrombosis: Basic Principles and Clinical Practice* (Colman, R. W., Hirsh, J., Marder, V. J., and Salzman, E. W., eds) pp. 1592–1622, J. B. Lippincott Co., Philadelphia, PA
14. Zahn, F. W. (1875) *Virchows Arch. Pathol. Anat.* **62,** 82–132
15. Riddle, J. M., and Barnhart, M. I. (1964) *Am. J. Pathol.* **45,** 805–823
16. Plow, E. F., Gramse, M., and Havemann, K. (1983) *J. Lab. Clin. Med.* **102,** 858–869
17. Plow, E. F. (1980) *Biochim. Biophys. Acta* **630,** 47–56
18. Plow, E. F. (1980) *J. Clin. Invest.* **69,** 564–572
19. Machovich, R., and Owen, W. G. (1990) *Blood Coagul. & Fibrinolysis* **1,** 79–90
20. Machovich, R., and Owen, W. G. (1989) *Biochemistry* **28,** 4517–4522
21. Morris, J. P., Blatt, S., Powell, J. R., Strickland, D. K., and Castellino, F. J. (1981) *Biochemistry* **20,** 4811–4816
22. Morris, J. P., and Castellino, F. J. (1983) *Biochim. Biophys. Acta* **744,** 99–104
23. Kolev, K., Komorowicz, E., Owen, W. G., and Machovich, R. (1996) *Thromb. Haemostasis* **75,** 140–146
24. Alkjaersig, N., Fletcher, A. P., and Sherry, S. (1959) *J. Clin. Invest.* **38,** 1086–1095
25. Matveyev, M. Y., and Domogatsky, S. P. (1992) *Biophys. J.* **63,** 862–863
26. Blinc, A., and Francis, C. W. (1996) *Thromb. Haemostasis* **76,** 481–491
27. Niewiarowski, S., Regoeczi, E., and Mustard, J. F. (1972) *Ann. N. Y. Acad. Sci.* **201,** 72–83
28. Loike, J. D., Sodeik, B., Cao, L., Leucona, S., Weitz, J. I., Detmers, P. A., Wright, S. D., and Silverstein, S. C. (1991) *Proc. Natl. Acad. Sci. U. S. A.* **88,** 1044–1048
29. Kolev, K., Léránt, I., Tenekejiev, K., and Machovich, R. (1994) *J. Biol. Chem.* **269,** 17030–17034
30. Tinker, D. O., Low, R., and Lucassen, M. (1980) *Can. J. Biochem.* **58,** 898–912
31. Henis, Y. I., and Yaron, T. (1988) *Biopolymers* **27,** 123–138
32. Teasdale, R. D., Carr, A. R., and Read, R. S. (1985) *J. Theor. Biol.* **114,** 375–382
33. Wang, D., Gou, S. Y., and Axelrod, D. (1992) *Biophys. Chem.* **43,** 117–137
34. Axelrod, D., and Wang, M. D. (1994) *Biophys. J.* **66,** 588–600
35. Gaspers, P. B., Gast, A. P., and Robertson, C. R. (1995) *J. Colloid Interface Sci.* **172,** 518–529
36. Carman, G. M., Deems, R. A., and Dennis, E. A. (1995) *J. Biol. Chem.* **270,** 18711–18714
37. Diamond, S. L., and Anand, S. (1993) *Biophys. J.* **65,** 2622–2643
38. Wu, J. H., Siddiqui, K., and Diamond, S. L. (1994) *Thromb. Haemostasis* **72,** 105–112
39. Anand, S., Wu, J. H., and Diamond, S. L. (1995) *Biotechnol. Bioeng.* **48,** 89–107
40. Sakharov, D. V., and Rijken, D. C. (1995) *Circulation* **92,** 1883–1890
41. Sakharov, D. V., Nagelkerke, J. F., and Rijken, D. C. (1996) *J. Biol. Chem.* **271,** 2133–2138
42. Wu, H. L., Shi, G. Y., and Bender, M. L. (1987) *Proc. Natl. Acad. Sci. U. S. A.* **84,** 8292–8295
43. Shi, G.-Y., and Wu, H.-L. (1988) *J. Biol. Chem.* **263,** 17071–17075
44. Deutsch, D. G., and Mertz, E. T. (1970) *Science* **170,** 1095–1096
45. Chase, T., and Shaw, E. (1970) *Methods Enzymol.* **19,** 20–27
46. Vindigni, A., and Di Cera, E. (1996) *Biochemistry* **35,** 4417–4426
47. Lowry, O. H., Rosebrough, N. J., Farr, A. L., and Randall, R. J. (1951) *J. Biol. Chem.* **193,** 265–275